ELEVENTH EUROPEAN ROTORCRAFT FORUM

Paper No 82

UK RESEARCH INTO SYSTEM IDENTIFICATION FOR HELICOPTER FLIGHT MECHANICS

G.D. Padfield
R. Thorne

Flight Research Division
Royal Aircraft Establishment
BEDFORD MK41 6AE, UK

D. Murray-Smith
C. Black
A.E. Caldwell

University of Glasgow

10-13 September 1985
LONDON, England

THE CITY UNIVERSITY, LONDON EC1V OHB, ENGLAND

UK RESEARCH INTO SYSTEM IDENTIFICATION FOR HELICOPTER FLIGHT MECHANICS

G.D. Padfield
R. Thorne

Royal Aircraft Establishment (BEDFORD)

D. Murray-Smith
C. Black
A.E. Caldwell

University of Glasgow

ABSTRACT

The techniques of system identification encompass a variety of processes in the derivation of input/output relationships using experimental data, including control input design, state estimation, model structure estimation and parameter identification. For helicopter flight mechanics studies, research is still required to develop a reliable system identification procedure that can be used with confidence at the design and development stages of a new project. UK research in this field is directed towards this aim with two principal objectives; firstly to develop a tool that can accurately gauge the validity and limitations of theoretical predictions methods, hence assisting the design process; secondly to provide a tool for use during development flight testing that can rapidly highlight problem areas and assist in establishing the degree of compliance with operational handling requirements.

This Paper reviews the status of a research programme in the UK from initial studies performed under an RAE/NASA collaboration through to the current collaborative activity between RAE Bedford and Glasgow University. The elements of the integrated process in use from control input design to model structure estimation are described and results using simulation and flight test data collected on the RAE research Puma are presented. The examples presented include the estimation of parameters affecting stability variations with flight path angle, highlighting aspects of the equation error, stepwise regression, model structure estimation process.

Finally the direction of future research is discussed, with reference to both analysis software and test facilities.

Nomenclature

a_x, a_y, a_z	aircraft acceleration components
F_{TOTAL}, F_i	total and partial F-ratios
g	gravitational acceleration
H_k	measurement equation transformation matrix
K_k	Kalman gain matrix
L_v, L_p etc	rolling moment derivatives

N_v, N_r etc.	yawing moment derivatives
P_k	error covariance matrix
p, q, r	aircraft roll, pitch and yaw rates
Q_k	process noise covariance matrix
R_k	measurement noise covariance matrix
R	multiple correlation coefficient
s_i	parameter standard deviation
u, v, w	aircraft translational velocity components
$\underset{\sim}{Y}_k$, $\underset{\sim}{W}_k$	measurement, process noise vectors
X	independent variable time history matrix
$x_1(t)$, $x_2(t)$ etc	independent variables
$\underset{\sim}{x}_k$	state vector
$\hat{\underset{\sim}{x}}_{n/m}$	estimate of $\underset{\sim}{x}$ at time t_n using observations up to time t_m
y(t), $\underset{\sim}{Y}$	dependent variable, vector
$\underset{\sim}{z}_k$	measurement vector
$\underset{\sim}{\varepsilon}(t)$	residual vector in regression equation
ζ, ω	dutch roll damping, frequency
η_p	pedal position
θ, ϕ, ψ	Euler pitch, roll, yaw angles
$\underset{\sim}{\theta}$	parameter vector
θ_0, θ_1, etc	unknown parameters in stepwise regression
θ_{0T}	tail rotor collective pitch
$\tilde{\underset{\sim}{\nu}}_k$	innovations vector
σ^2	parameter variance
Φ_k	transition matrix

1 INTRODUCTION

In a broad range of scientific disciplines, the need to derive a mathematical formulation of the behaviour of a system based on measurements of the response to a range of inputs, has led to the development of system identification analysis tools. The presence of measurement and process noise in most real systems has a profound effect on the performance of identification methods requiring that a statistical rather than deterministic formulation be adopted. A variety of sub-problems emerges as a result of the uncertainties caused by imperfect data, including input design, state estimation, model structure estimation and parameter identification. The integration of these processes and the application to helicopter flight dynamics is the subject of this Paper.

System identification techniques fulfil two main functions in the design and development of new aircraft; firstly, validation and improvement of predictive theoretical models through comparison with model structure and parameters estimated from measurements on existing vehicles, provide a measure of confidence in the design tool. Secondly, during development flight testing, measurements made during clinical flying qualities tests can be used to estimate stability and control and handling parameters of interest, for demonstrating compliance with requirement specifications or to upgrade the design simulation. These functions are equally valid for research investigations. A further application, yet to be fully exploited, involves the use of on-line identification to realise the full potential of adaptive flight control.

As an aid to the design and development process, system identification methods should possess robust properties particularly to noise statistics; ease of use is also important with clear indications of confidence levels, hence likely accuracy and sensitivity to errors. Powerful statistical techniques now exist that confer reliability properties on modern estimation algorithms and a long history of successful applications to fixed wing aircraft[1] has provided the confidence necessary for their routine use, at least for flight régimes where the usual linearity assumptions are valid. The number of applications to helicopters has been significantly fewer[2-19] and within these, the number of successes small. This does not mean that the techniques are necessarily inadequate, but more that a number of features peculiar to helicopters combine to make their application considerably more complicated. These include,

(a) system complexity - coupled longitudinal/lateral dynamics, interaction with rotor dynamics

(b) high vibration environment - reducing signal to noise ratio

(c) instabilities - restricting data record lengths, difficulty in trimming

(d) nonlinearities - moderate sized inputs required because of (b) leading to airspeed/sideslip/incidence nonlinear effects

(e) air data measurements sensitive to rotor wake and fuselage flow field effects

Previous studies[4,7,14] have highlighted identification difficulties associated with these factors that have led, for example, to gross underestimation of damping derivatives and poor estimates of cross coupling effects.

Taking account of these special difficulties, a number of integrated approaches have been developed for helicopters[1,4,10,15] and this Paper outlines the collection of tools being created at RAE Bedford in collaboration with Glasgow University. Section 2 reviews the background to the UK activity from initial studies

carried out under an RAE/NASA collaborative programme through to current studies within the UK, including a detailed description of the RAE developed software package PEP (Parameter Estimation Package). Methodology validation using data from simulation models is treated in section 3 and followed by an example of flight data analysis in section 4. Current and future developments of the approach are described in section 5.

2 UK RESEARCH PROGRAMME

2.1 Background

The principal aim of the research in this field in the UK is the validation of theoretical prediction models, or, more specifically, the definition of the areas of validity of different levels of modelling for flying qualities investigation. Validation, in turn, determines the level of confidence that can be ascribed to results from control system design studies on the one hand, and to the effects of vehicle design changes on the other. In the exploration of a new concept, some extrapolation beyond the database used for the validation is usually necessary, in terms of flight envelope, aircraft configuration and control response. This situation is inevitable, but the associated uncertainties can be minimised by establishing and calibrating the accuracy of modelling at the limit of the available database.

Modelling of rotorcraft flight behaviour and the associated loadings can conveniently be partitioned into three distinct levels, differentiated largely by the form of rotor modelling, as summarised in Table 1. Level 1 modelling includes the 'rigid body' six degree of freedom linear or nonlinear formulation with quasi-steady rotor dynamics and extends to the inclusion of rigid rotor blade (multiblade coordinate) dynamics with analytically integrated blade loadings, together with a range of additional dynamic elements *eg* engine/rotorspeed, actuators. Aerodynamic inflow representation in Level 1 modelling extends from the uniform 'momentum' component plus a linear variation across the disc, to a dynamic inflow representation[20].

Level 1 models are useful for flying qualities and performance studies within the normal flight envelope where integrated rotor loads are not significantly effected by rotor stall, compressibility effects and the attendant rotor blade dynamic couplings. They provide the basis for practically all of the piloted simulation research conducted to date[20,21]. Level 3 modelling, at the other extreme, represents the most comprehensive rotor/fuselage modelling necessary to predict not only integrated, but also vibratory loadings across a wide bandwidth where rotor couplings and nonlinear aerodynamic effects can be significant. Detailed structural representation of the blade dynamics and the induced flowfield through and below the rotor are required and result in models of considerable complexity that are slow to run even on powerful computers[22,23]. Between these two extremes of complexity lie a range of modelling options that are now being considered for the upgrading of real time piloted simulations. One of the most important reasons for establishing a viable Level 2 model is the need to explore the design implications for high gain

active control systems[24] in a piloted simulation environment. Increased exploitable primary flight control bandwidth, and flight in conditions where aerodynamic nonlinearities and rotor couplings prevail, require that both the dynamic and aerodynamic rotor modelling is enhanced relative to Level 1 models. Individual blade dynamic models with loadings integrated numerically around the azimuth and along radial blade elements are, in fact, already being configured to run in real time[25], albeit with a much simplified representation of the rotor inflow compared with Level 3 models. Research is still needed to derive a more realistic inflow distribution for Level 2 models.

Helicopter system identification research in the UK has, to date, concentrated on the validation of Level 1 models. Time history correlation of flight and simulation data[20] in support of a series of 'agility' simulation trials conducted at RAE in the late 1970s indicated some serious discrepancies, particularly in cross coupling effects, even though qualitatively, pilots felt the total simulation to be realistic. A more systematic approach to validation was clearly required and a TTCP (The Technical Cooperation Programme) collaboration was initiated between the NASA Ames Research Center and the RAE Bedford to exchange flight data and techniques for rotorcraft system identification. The first phase of the collaboration included a workshop held at Ames[26] when RAE Puma data was processed by elements of a suite of NASA programs developed in support of the Rotor Systems Research Aircraft programme. Results from the first phase were eventually reported in Ref 14 and included model structure estimates for aircraft angular motion at a single flight condition. The results of the first phase were encouraging although low estimates of roll damping and curiously high cross coupling derivatives were not fully resolved. The collaboration continued with an exchange of estimation and simulation software enabling both agencies to continue development of the process in parallel. Since that time research at the RAE has focussed on the development of an integrated methodology through the creation of PEP, as illustrated in Fig 1. For the last two years the activity has been strongly supported by the University of Glasgow principally in the areas of control input design and estimation in the frequency domain.

2.2 PEP and the integrated methodology

The following discussion refers to the various stages in the integrated process illustrated in Fig 1 and describes how these have been implemented in PEP (Fig 2).

2.2.1 Control input design

Test input selection and experimental design considerations are known to be particularly important in aircraft applications[1]. In practical terms, some of the factors which have to be considered in the design of flight test procedures for system identification purposes include questions of safety and pilot acceptability. The selection of test conditions which ensure that the measured responses show adequate sensitivity to the main parameters of interest, and careful consideration of the forms of perturbation

which can be tolerated in relation to the modelling assumptions (such as linearity) implicit in the identification process, are additional factors. The particular problems of system identification and related test input design for helicopters have been covered in the introduction to this Paper. Because of the large number of coupled degrees of freedom, the success of parameter estimation techniques tends to be particularly limited by the information content of the data in relation to the number of unknown parameters.

From both theoretical and practical points of view, a class of test inputs that offer favourable properties in terms of bandwidth and discrimination against noise is the psuedo-random binary sequences (multi-step functions). Such signals are periodic and have an impulsive type of auto-correlation function which approximates that of band limited white noise. The number of zero crossings within the period of a pseudo-random binary sequence is 2^{r-1} where r takes the integer values 2, 3, 4 etc. In practice, the test signals of this nature used in flight work are limited to small values of r and only one cycle of the periodic signal is applied. For example, the widely used 3211 test input is a single cycle of a pseudo-random signal which can be generated for $r = 3$. The continuous spectrum for this input, shown in Fig 3 reveals features associated with the discrete spectrum of the periodic sequence, for example, the node at $\omega = 2\pi$ rad/s and the 0.9 rad/s spectral line separation.

For pilot inputs, the high frequency components are limited by the maximum rate of movement possible on the controls. Fig 3 also shows a record of a pilot applied 3211 test input together with the corresponding spectrum estimate. The restrictions on pilot applied inputs are clearly not very serious for the bandwidth shown. The use of longer test sequences is severely limited for helicopters by divergent aircraft response characteristics. Nevertheless, the well defined properties of binary test signals do provide a useful theoretical framework for control input design with the selection of spectral modes and line separation allowing broad based excitation together with emphasis at particular frequencies.

Control input design algorithms for application to helicopter flight testing are currently the subject of a research study, conducted at the University of Glasgow, based on the multi-step binary sequences applied to a nonlinear helicopter simulation model. Algorithms being investigated include a scheme whereby the input design is cast as a two-point boundary value problem where the control sequence is chosen to minimise parameter estimation errors, *eg* weighted sum of dispersion matrix diagonal elements[10]. Results from these studies will be applied in a forthcoming flight trial at RAE Bedford.

The flight database[27] built up over the last few years at RAE consists primarily of responses to 3211 multi-steps, doublet and step inputs applied over a wide range of flight conditions. The results described in this Paper are drawn from this collection.

2.2.2 Flight tests

The current flight test vehicle at RAE Bedford used for system identification work is the general purpose research Puma (Fig 4). A brief description of the aircraft and its digital (PCM) data acquisition system was given in Ref 14. The aircraft is comprehensively instrumented with high quality sensors for inertial data (acceleration, rates, attitudes), air data (airspeed, incidence angles), rotor motion data (blade flap, lag, pitch angles, rotorspeed) and pilot control inputs. Data acquisition rates vary with requirements but generally range from 32/s for slowly varying quantities to 256/s for rotor blade root angles. Overall data rate is also programmable and can be increased to a maximum rate of 128K 16 bit words per second for the measurement of rotor blade pressure distributions.

Flight testing for system identification work requires careful piloting to set up trim conditions accurately and to apply control inputs in a precise and repeatable fashion. Normally three runs at each test point and control input are recorded, with additional inputs applied at increasing amplitudes to enable linearity checks to be performed. Depending on the stability of the trim state being perturbed, record time for a return-to-trim multi-step control sequence will vary between 10-30 s.

Following a flight, the data tape is processed and data transferred to computer compatible tape. The EDSTRACT file creation programme (Fig 2) applies calibration factors to convert to engineering units, merges data with ground based recordings (*eg* kinetheodolite data), and creates disk files of individual runs. At both RAE Bedford and Glasgow University, the analysis software is currently implemented on a VAX computer system.

2.2.3 Preliminary data interpretation

Important features of response characteristics can be observed through a preliminary interpretation and comparative check on the data. This process should cover repeatability, linearity and enable rough estimates to be derived of damping, frequencies, control sensitivities and the levels of cross coupling involved. In addition, an assessment of the kinematic consistency of sensor data can be made. This enables estimates to be made of any likely calibration errors and is now a fairly standard procedure in flight data analysis[28-30]. The kinematic equations of translational motion and associated Euler equations of rotational motion form the basis of the estimation model.

$$\dot{u} = -wq + vr + a_x - g\sin\theta \qquad (1)$$

$$\dot{v} = -ur + wp + a_y + g\cos\theta\sin\phi \qquad (2)$$

$$\dot{w} = -vp + uq + a_z + g\cos\theta\cos\phi \qquad (3)$$

$$\dot{\phi} = p + q\sin\phi\tan\theta + r\cos\phi\tan\theta \qquad (4)$$

$$\dot{\theta} = q\cos\phi - r\sin\phi \quad (5)$$

$$\dot{\psi} = q\sin\phi\sec\theta + r\cos\phi\sec\theta \quad (6)$$

Here u, v, w are the translational velocity components; p, q, r the angular velocities, ϕ, θ, ψ the Euler angles and a_x, a_y, a_z the translational accelerations. Using rate gyro and accelerometer measurements, estimates of velocities and Euler angles can be made from the above differential equations for comparison with measurements from the air data and attitude sensors. Fig 5 illustrates results obtained from the KINECON option in PEP (Fig 2) showing the comparisons described above for a pedal doublet response at 100 kn. Velocity estimates indicate the possibility of bias errors in the accelerometer calibrations. Bias estimates can be derived in KINECON using a weighted least squares output-error algorithm and Fig 5 also shows the improvement in the comparison of the velocity components u and w when these are included. Regular checking of instrument calibration factors in this way minimises the effort expended in later processes.

The PREPLOT facility shown in Fig 2 allows the user to perform a number of useful time series manipulative functions including direct comparison with simulation data. Figs 6 and 7 illustrate the Puma response to longitudinal and lateral cyclic 3211 inputs at 80 kn. HELISTAB[31,32] simulation results (before upgrading) are shown as the broken lines, and although some principal features are in agreement there are some significant differences. Dutch roll period and damping appear to be higher in the simulation than in flight although relative magnitudes in Fig 7 are in reasonable agreement. Coupling effects in Fig 6 are stronger in the simulation with noticeable sideslip, hence roll and yaw excursions. Many of these anomalies were first discussed in Ref 14 where the yawing moment due to incidence N_w was shown to cause the increased sideslip response to pitch motion, and reduction in dutch roll damping in the simulation model. The differences between flight and simulation results were attributed partly to unmodelled rotorspeed and engine torque degrees of freedom.

2.2.4 State estimation

The fourth stage in the process highlighted in Fig 1 involves the computation of filtered or smoothed state estimates from the measurements. With the aircraft kinematic equations (1-6) forming the system model in an extended Kalman filter algorithm, calibration factors can be fully revised, unmeasured states estimated and the levels of measurement noise on the data reduced. The technique is particularly sensitive to the assumed process noise statistics, or the uncertainty in the validity of the system model. Atmospheric disturbances and unmodelled degrees of freedom will contribute to the process noise. This stage is performed in PEP by the program DEFKIS (Discrete Extended Kalman Filter/Smoother[10]), one of the software elements acquired from NASA under the original RAE/NASA collaborations. The extended Kalman filter linearises the system equation about each time point t_k, in the discrete form,

$$\underset{\sim}{x}_k = \Phi_k \underset{\sim}{x}_{k-1} + \underset{\sim}{w}_{k-1} \tag{7}$$

with the corresponding linearised measurement equation,

$$\underset{\sim}{z}_k = H_k \underset{\sim}{x}_k + \underset{\sim}{v}_k \tag{8}$$

Here $\underset{\sim}{x}_k$ and $\underset{\sim}{z}_k$ are the state and measurement vectors respectively, Φ_k is the transition matrix, H_k the measurement matrix, and $\underset{\sim}{w}_k$ and $\underset{\sim}{v}_k$ the process and measurement noise respectively, with assumed statistical properties (mean and covariance[33]).

$$\underset{\sim}{w}_k \sim N\left(\underset{\sim}{0}, Q_k\right) \tag{9}$$

$$\underset{\sim}{v}_k \sim N\left(\underset{\sim}{0}, R_k\right) \tag{10}$$

The filter equations then take the form:

$$\hat{\underset{\sim}{x}}_{k/k} = \hat{\underset{\sim}{x}}_{k/k-1} + K_k \underset{\sim}{\nu}_k \tag{11a}$$

$$\hat{\underset{\sim}{x}}_{k+1/k} = \Phi_k \hat{\underset{\sim}{x}}_{k/k} \tag{11b}$$

$$\underset{\sim}{\nu}_k = \underset{\sim}{z}_k - H_k \hat{\underset{\sim}{x}}_{k/k-1} \tag{12}$$

$$K_k = P_{k/k-1} H_k^T \left[H_k P_{k/k-1} H_k^T + R_k\right]^{-1} \tag{13}$$

$$P_k = \left[1 - K_k H_k\right] P_{k/k-1} \tag{14}$$

$$P_{k/k-1} = \Phi_{k-1} P_{k-1} \Phi_{k-1}^T + Q_{k-1} \tag{15}$$

In equation (11)-(15) the filtered state estimate $\tilde{x}_{k/k}$ is calculated as a sum of the model estimate and a feedback term from the innovations $\tilde{\underset{\sim}{\nu}}_k$ with gain matrix K_k. The gain matrix is updated in each time cycle based on the error covariance update $P_{k/k-1}$. The scheme is simplified as a feedback system in Fig 8, illustrating the filter-nature of the process. At the two extremes, (low Q_k, high R_k; high Q_k, low R_k), the filter outputs the model response and measurements respectively as the resulting 'best estimate'. In practice, the measurement noise can usually be specified reasonably accurately, based on the standard deviation of the noise on the various measurement records. The process noise is, to some extent, a mathematical artifact introduced to enable the Kalman filter formulation to be used and hence the associated covariance is less easy to define. The 'best' values may well vary from run to run and some iteration may be required before filter convergence is achieved. This aspect makes the filter somewhat hard to tune for the general case and sometimes even for particular cases, especially where velocity component excursions are large and

significant differences between airdata and integrated accelerometer measurements can occur. Combining the estimates from a forward filter run with a backward filter run enables a smoothed estimate to be derived with lower variants than either of the filter estimates[33].

Fig 9 (PLOTDEK graphics) shows a comparison of original flight measurements with filter and smoother estimates for the pedal doublet run referred to earlier (Run 467/10/11). The extracted noise time histories are also shown (*ie* $\underset{\sim}{z} - \underset{\sim}{\hat{z}}_{\text{smoother}}$).

A typical DEKFIS run will use measurements from rate and attitude gyros, accelerometers and airspeed probe and incidence vanes, and compute smoothed estimates of the measurements together with velocity components and angular accelerations. The programme PERTURB shown on Fig 2 offers the option for deriving perturbation time histories about the nominal trim point.

2.2.5 Model structure estimation (MSE)

This stage in the process utilises the computationally efficient step-wise regression algorithm to estimate first approximations to the parameter estimates in a class of model structures. The technique has regained prominence in aircraft system identification in recent years, not only to provide starting values for maximum likelihood output error estimation but also as a means of exploring the ability of different linear and nonlinear model structures to fit flight measurements[34,35]. The estimation can be performed in the time or frequency domain, hence the option of the fast Fourier transform (FFT) in Fig 1. Frequency domain estimation has the advantage that the model fit can be restricted to a defined frequency range, enabling reduced order models to be derived for either single input/single output transfer functions[17,18], or multi-degree of freedom models[14]. Although not shown in Fig 2, the option now exists in PEP to derive FFTs of the measurements and smoothed states at the DEKFIS/ PERTURB output stage or initially on the EDSTRACT files. The use of this option is currently being explored at Glasgow University with simulation data including rotor dynamics, and results will be reported at a later date. The analysis of flight data in this Paper is carried out largely in the time domain.

The Optimal Subset Regression (OSR - acquired through RAE/NASA collaboration) program, shown in Fig 2, formulates the equation error as a least squares minimisation problem. Thus,

$$y(t) = \theta_0 + \theta_1 x_1(t) + \theta_2 x_2(t) + \ldots . \varepsilon(t) \qquad (16)$$

or

$$\underset{\sim}{y} = X \underset{\sim}{\theta} + \underset{\sim}{\varepsilon} \qquad (17)$$

where the elements of the vector $\underset{\sim}{y}$ are the estimates of the dependent variable at the discrete time points and the matrix X is made up of the time histories of the independent variables x_1, x_2 etc, arranged as columns. The residual vector $\underset{\sim}{\varepsilon}(t)$ represents a combination of measurement noise on the dependent state $y(t)$ and any additional process noise.

θ_o represents any bias or trim residual and $\theta_1 \ldots . \theta_n$ represent the stability and control derivatives, including higher order terms in a Taylor expansion for the most general nonlinear case. The least squares solution for the parameter vector $\underset{\sim}{\theta}$ is given by

$$\hat{\underset{\sim}{\theta}} = (X^T X)^{-1} X^T \underset{\sim}{y} \tag{18}$$

The properties of this solution are well documented[36]; the estimates will be unbiased, provided that the independent variables are free from measurement noise, and the measurement noise on the dependent variable and the process noise have zero mean. If, in addition, these noise sources are white, then the parameter covariance matrix can be written

$$\text{COV}\left(\hat{\underset{\sim}{\theta}} - \underset{\sim}{\theta}\right) = \sigma^2 (X^T X)^{-1} \tag{19}$$

where σ^2 is the variance of the equation error. Flight data does not, in general, satisfy the above conditions so that the residual may have a deterministic component and needs to be examined for such. Despite these drawbacks (asymptotically biased, inconsistent and inefficient), provided measurement noise has been filtered out, the accuracy of the method is often comparable with more sophisticated output-error methods[34].

The stepwise regression procedure applies the least squares fit in a sequence of steps, each time adding or deleting an additional independent variable to the regression equation until a best fit is obtained. At any stage in the process the variable chosen for entry to the regression will have the highest partial correlation with the residual (or highest partial F_{enter} statistic). The multiple correlation coefficient R is a direct measure of the accuracy of the fit, while the total F-ratio provides a measure of the confidence one can ascribe to this fit. The partial F-ratios for individual parameters also provide individual confidence measures. These fit criteria can be expressed as:

$$R^2 = \frac{(X\hat{\underset{\sim}{\theta}})^T (X\hat{\underset{\sim}{\theta}})}{\underset{\sim}{y}^T \underset{\sim}{y}} \tag{20}$$

$$F_{TOTAL} = \frac{R^2/(p-1)}{(1-R^2)/(m-p)} \tag{21}$$

$$F_i = \hat{\theta}_i^2 / s_i^2 \tag{22}$$

Here p is the number of parameters in the fit, m the number of time points and s_i, the standard error of the parameter θ_i. Both R^2 and the F-ratios have to be tracked during a regression run to establish the maximum total and partial

F-ratios; R^2 will, by definition, continue to increase with each new parameter added. The regression will stop when either R^2 attains a pre-defined value or the individual F-ratios of remaining parameters fall below a specified critical value.

Following on with the pedal doublet example described earlier, OSR runs were made to derive the coefficients in the yawing and rolling moment equations, thus,

$$\dot{r} = N_v v + N_r r + N_p p + N_{\eta p} \eta_p + ... \quad (23)$$

$$\dot{p} = L_v v + L_r r + L_p p + L_{\eta p} \eta_p + ... \quad (24)$$

Derivative estimates were made for both the free response portion of the data (320 points) and the total range (480 points). The F-ratio threshold was set low (1.0) to allow effects of insignificant parameters to be explored. Figs 10 to 13 show the stepwise results of this study. For both yawing and rolling accelerations, only the first few steps in the process are plotted; generally speaking, as soon as the longitudinal coupling derivatives are entered into the fit equation, the confidence level on the primary stiffness (N_v , L_v), damping (N_r , L_p) and control ($N_{\eta p}$, $L_{\eta p}$) derivatives reduces markedly. The reduced order models give the best fit for the smallest number of parameters. The breakdown in confidence (or increase in parameter variance) at relatively low order model structures can be attributed partly to the linear dependence of aircraft angular motions, particularly roll and yaw, more evident in the lightly damped dutch roll oscillation (see Ref 1, Paper No 6). How the parameter estimates and this reduced model structure compare with simulation model predictions will be discussed in section 4. Performing stepwise regression on an increasing time span of data allows the derivative estimates in a defined model structure to be plotted against manoeuvre time as shown in Fig 14. The derivatives are seen to have approximately converged after only 10 s into the manoeuvre, *ie* after only 2 to 3 cycles of the oscillation. It is important to conduct this convergence test, which, if fulfilled, tends to guarantee the prediction quality of the model at least for the single run being explored. Fig 15 shows the reconstructed yaw (r) and roll (p) accelerations compared with the original smoothed estimates, together with the residuals. Although the yaw residual appears to have random properties there are clear deterministic features in the roll residual. The dominant frequency in the residual is also twice that of the primary response, suggesting some form of nonlinearity, although the error is still quite small. Fig 16 illustrates the predictive quality of the model structure for roll/yaw motion; here the derivatives are applied to an opposite pedal doublet run carried out during the same flight. As expected, the fit is reasonable, although a slight drift in the reconstructed roll acceleration detracts from an otherwise close agreement. These results are returned to again in section 4.

2.2.6 Parameter identification

Model structures and associated parameter values estimated at the MSE stage can be used finally as a starting point for output error, maximum likelihood identification[1] which iterates towards unbiased, minimum variance estimates and provides information on the associated reliability and uncertainty levels. For all possible combinations of unknown parameter values, this process selects that which maximises the probability density function of the observations - hence maximum likely values. The scheme is now widely used and probably accepted as the most optimal and flexible for use in aircraft dynamics. However, application to helicopters have been plagued with problems, largely, it is believed, because the validity of essential model structures has not been checked. Hence, even though the variances of the estimates approach their lower bound for long records, the actual estimates at any given time point may or may not have any physical significance. The use of output error, maximum likelihood techniques for helicopter system identification in the UK to date has been minimal. Analysis tools are, however, currently being incorporated into PEP and experience should be gained within the near future.

3 METHODOLOGY VALIDATION

In Fig 1 the use of a simulation model to validate the methodology is stressed. The effects of measurement noise, degrees of freedom, nonlinearities, record length and other aspects on the various processes, can be explored in a controlled fashion and used to guide the decision making logic when processing flight data. The simulation model currently used at RAE and Glasgow is the flight mechanics package HELISTAB[31,32], an RAE Level 1 model with options for a range of different rotor degrees of freedom. Both measurement and process noise *(eg* gusts) can be built into a simulation run for methodology validation work.

Many of the problems associated with identifying linear models from nonlinear simulation data can be calibrated and have been shown to re-appear in flight data analysis. Fig 17, for example, illustrates the variation in estimated yawing moment derivatives, from a lateral cyclic 3211 manoeuvre, with control amplitude. Two step clock periods are shown, 0.5 s and 1.0 s, and the derivative estimates are normalised by the small perturbation HELISTAB predictions. Damping and coupling derivative estimates are departing markedly from the linear approximation as control input and clock period increase. Both these factors increase the nonlinear excursions in the response variables. An even more dramatic effect is shown in Fig 18 where the yaw damping is plotted against step number (from an OSR run); the control input for this HELISTAB run is a pedal doublet, and the flight speed 80 kn. The variation of the F-ratio for N_r and N_p (F_{remove} given by equation (22)) reveals the vital importance of tracking these quantities during the regression. The maximum partial F-ratio comes at the 5th step and beyond the 6th step the estimated values for both N_r and N_p are totally unrealistic. The fit error however has continued to decrease. These examples endorse earlier findings that it may only be possible to obtain good estimates for a limited model structure in any given case. The evidence suggests that the kind of problem

highlighted above is not simply a question of control input design; the same F-ratio statistic collapse occurs with a 3211 input. Current studies include the estimation of nonlinear model structures from simulation data and form an essential part of methodology validation.

4 LATERAL/DIRECTIONAL STABILITY VARIATION WITH FLIGHT-PATH ANGLE

The variation of dutch roll damping for the Puma with flight-path angle is quite marked. Fig 19 illustrates the effect showing the response to a pedal doublet input in descent (~ 1000ft/min), level and climbing flight (~ 1000 ft/min) at a 100 kn trim condition. The results shown are smoothed estimates obtained from the state estimation process described in 2.2.4 and include the estimated yaw and roll accelerations. As can be seen from the figure, stability is eventually lost in climbing flight. The level flight case has already been discussed in section 2 where it was shown that model structures for rolling and yawing motions need to be confined to the primary stiffness, damping and control terms for sensible results. A similar collapse of the F-ratio statistics occurs for all three flight conditions and Fig 20 illustrates the variation of estimated derivatives for the reduced model structure. Included in the figure are estimates of the static stability derivatives N_v and L_v from steady heading sideslip tests, and the HELISTAB predictions. Noticeable features of the comparisons are:

(a) Much lower N_v values predicted by the simulation. Increasing the perturbation size in the computational scheme for obtaining the simulation derivatives produces higher values of N_v, (to about 80% of flight estimates for similar excursions), indicating a nonlinear effect with sideslip. This can be attributed to the fin aerodynamics and is discussed in more detail in Ref 14.

(b) Simulation model predicts sensibly constant yaw damping, N_r, whereas flight estimates vary significantly. This can be attributed to the fact that the OSR process has effectively lumped all the system damping into this derivative and, although the standard deviation is small, experience suggests that the flight values are not physically meaningful, and that effects other than yaw damping per se, are contributing to the motion.

(c) The increasing dihedral effect ($-L_v$) with flight path angle is more significant in the flight estimates. This effect is likely to be one of the main factors in the loss of stability with climb angle.

(d) Roll damping is estimated from flight data to be only 70-80% of the simulation prediction. We can expect this to

be another lumped effect, but without any information on the rolling moments due to yaw and pitch rate, further speculation at this stage is futile.

(e) Both control derivatives are overpredicted by theory by a substantial amount. Included in Fig 20 are estimates of the control derivatives using tail rotor pitch actuator response data rather than pedal position. The improvement in the comparison with theory is significant but flight estimates are still only of the order of 70% of theoretical prediction. The simplifying assumptions in the tail rotor modelling *ie* simple actuator disc representation) are almost certainly the cause of this anomaly.

Apart from the more obvious effects of increased dihedral and reduced roll damping, the comparisons described above have shed little light on the mechanism behind the variation of dutch roll damping with flight path angle. A further step can be taken in this direction however if the damping is assumed to take the approximate form[37],

$$\zeta = \frac{1}{2\omega} \left\{ -N_r + N_p \left(\frac{L_r}{L_p} - \frac{VL_v}{L_p^2} \right) \right\} \qquad (25)$$

where ω is the dutch roll frequency and V is the flight speed. If we make the further assumptions that,

$$\left| L_r \right| << \frac{VL_v}{L_p} ,$$

then the effective yaw damping can be written as,

$$N_{r_{effective}} \sim N_r + N_p \frac{VL_v}{L_p^2} \qquad (26)$$

Using the theoretical predictions for N_r (~ -0.5) in (26), we can derive values for the coupling derivative N_p by substituting for the flight estimates, from OSR, of L_v, L_p and N_r (for N_r effective) with N_p fixed at zero. The estimates of N_p are compared below with simulation predictions.

	N_p (Flight)	N_p (HELISTAB)
Descent	-0.213	-0.227
Level	-0.246	-0.21
Climb	-0.295	-0.19

Although the trend with flight path angle is predicted incorrectly, the comparison is reasonable, giving some confidence that this adverse yaw is the missing effect. The theoretical prediction of N_p is largely due to the product of inertia I_{xz}, coupling rolling with yawing motion. The phase and amplitude relationship between roll and yaw motion, illustrated in Fig 19, does confirm the overall effects of adverse yaw on this aircraft. In particular, the increasing roll/yaw ratio with climb angle shown in the flight results, supports the destabilising effect of increased dihedral in the presence of adverse yaw. Creating a new lateral/directional linear sub-system with flight estimated derivatives replacing HELISTAB predictions where appropriate, leads to the following values for the dutch roll eigenvalue, compared with the original HELISTAB prediction.

	HELISTAB	New lateral sub-system
Descent	-0.106 + 0.9i	-0.17 + 1.37i
Level	-0.057 + 0.94i	-0.118 + 1.53i
Climb	-0.037 + 0.94i	0.052 + 1.45i

The new model structure correctly predicts the instability, as expected, and of course, the total system damping is now shared between the two effects expressed in (26). In addition, the frequency is now much closer to the flight value.

The arguments developed above are reasonable but not conclusive, and it is clear that more reliable estimation procedures together with improved control input designs are desirable and required to refine the model structures directly from the flight data. In particular, methods are required which are able to isolate the contributions of the various cross coupling effects, hence allowing expanded model structures with continued decrease of parameter variances *(ie* increase in partial F-ratios).

5 FUTURE RESEARCH

As pointed out in the Introduction to this Paper, the main effort in the UK in the short term is being directed towards mapping out the areas of validity of Level 1 modelling together with indications of the model deficiencies where the flight test results have been able to highlight these. The results presented in this Paper are typical of a set that are currently being catalogued for the Puma aircraft across a range of flight conditions. During the next year or so, it is planned that data from at least three other aircraft types will be added to the database allowing system identification analysis and correlation studies to be carried out for different vehicle configurations. This will include experiments carried out on the RAE Research Lynx for which an optimal control input device is currently being developed[38]. This system will allow pre-programmed control inputs to be applied directly to the flight control system limited authority series actuator. In the same time frame it is planned to initiate studies into the validation of

Level 1 multi-blade coordinate, rotor-dynamic models, using measurements of rotor-blade-root flap and pitch angles. Additional measurements made on a specially instrumented blade, with incidence indicating pressure transducers along the leading edge, will allow more detailed model correlation leading eventually to validation studies with Level 2 models.

Current developments underway to improve the identification methodology include frequency domain analysis, multiple run analysis which is shown in Ref 1 (Paper 7) to offer several advantages to the estimation process, a more systematic and rational approach to control input design, nonlinear model structure estimation and, finally, the use of maximum likelihood parameter identification.

6 CONCLUSIONS

A research programme into the application of system identification methods to helicopter flight mechanics in the UK has been outlined. The need for an integrated methodology has been stressed including control input design, state estimation and model structure estimation processes. Elements of the principal computer analysis tool, the Parameter Estimation Package, have been described with sample results presented using measurements made on the RAE Research Puma. The use of a simulation model to conduct validation studies on the methodology itself has been emphasised, not only to improve the understanding of the various stages, but also to highlight difficulties common with the analysis of flight data and, in some cases, how to overcome these. The example presented of the response to a pedal doublet is a case in point, where it has been shown necessary, for both flight and simulation data, to restrict the estimated model structure to simple lateral and directional motions. Variations in the stability of the dutch roll mode with flight path angle were explored in some detail. Initially, the simulation model was unable to predict the important effects but a reduced order upgraded model derived from the flight data has shed light on the mechanism behind the growing instability with climb angle. Future aspects of the continuing research programme in the UK have been briefly described. These include developments in the methodology to improve its robustness, reliability and efficiency and effort is currently being directed to overcome the system identification problems, peculiar to helicopters, highlighted in this Paper.

Major improvements in the reliability of system identification methods for helicopter applications are still required before they are available for routine use during design and flight test development. Although successes have been claimed, the greater number of published cases where dampings have been grossly underestimated and cross couplings poorly predicted suggests that considerable specialist effort is required to overcome problems peculiar to helicopters. This is a research task, and more fundamental studies with elements of the structured approach described in this Paper are urgently required.

Table 1

	Level 1	Level 2	Level 3
AERODYNAMICS	Linear 2-D - dynamic inflow/local momentum theory - analytically integrated loads	Nonlinear (limited 3-D) - dynamic inflow/local momentum theory - local effects of blade/vortex interaction - unsteady 2-D - compressibility - numerically integrated loads	Nonlinear (3-D) - full wake analysis (free or prescribed) - unsteady 2-D - compressibility - numerically integrated loads
DYNAMICS	i Rigid blades - 6 dof quasi steady rotor - 9 dof - rotor flapping - 12 dof - flap + lag - 15 dof - flap + lag + pitch	i Rigid blades options as in Level 1 ii Limited number of blade elastic modes	i Elastic modes (detailed structural) representation
APPLICATION	- parametric trends for flying qualities/performance studies - within operational flight envelope - low bandwidth control	- parametric trends for flying qualities/performance studies - beyond operational flight envelope - medium bandwidth appropriate to high gain active flight control	- rotor design - rotor load prediction across a high bandwidth - beyond operational flight envelope

REFERENCES

1) Parameter Identification. AGARD LS-104, Nov. 1979.

2) J.A. Molusis, Helicopter stability derivative extraction and data processing using Kalman filtering techniques. 28th AHS National Forum, Washington, (1972).

3) J.A. Molusis, Helicopter stability derivative extraction from flight data using the Bayesian approach to estimation. Journal of the AHS, July 1973.

4) J.A. Molusis, Rotorcraft derivative identification from analytical models and flight test data. AGARD CP 172 'Methods for aircraft state and parameter identification', Nov. 1974.

5) D.G. Gould, W.S. Hindson, Estimates of the lateral-directional stability derivatives of a helicopter from flight measurements. NRC Aero Report LR-572, Dec. 1973.

6) J. Kaletka, O. Rix, Aspects of system identification of helicopters, 3rd European Rotorcraft Forum, Aix-en-Provence, Sept. 1977.

7) O. Rix, H. Huber, J. Kaletka, Parameter identification of a hingeless rotor helicopter. 33rd AHS National Forum, May 1977.

8) W. Earl Hall Jr, N.K. Gupta, R.S. Hanson, Rotorcraft system identification techniques for handling qualities and stability and control evaluation. 34th AHS National Forum, Washington, May 1978.

9) M. Kloster, J. Kaletka, H. Schaufele, Parameter identification of a hingeless rotor helicopter in flight conditions with increased instability. 6th European Rotorcraft Forum, Bristol, Sept. 1980.

10) W.E. Hall Jr, J.G. Bohn, J.H. Vincent, Development of advanced techniques for rotorcraft state estimation and parameter identification. NASA CR 159297, Aug. 1980.

11) W. Hodge, Comparison of analytical and flight test identified derivatives for a tandem rotor transport helicopter. NASA TP-1581, (1980).

12) R.W. DuVal, The use of frequency methods in rotorcraft system identification. 1st AIAA Flight Testing Conference, Paper 81-2386, Las Vegas, Nov. 1981.

13) R.W. DuVal, D.B. Mackie, Identification of a linear model of rotor-fuselage dynamics from nonlinear simulation data. Vertica, Vol. 5, 1981.

14) G.D. Padfield, R.W. DuVal, Applications of system identification to the prediction of helicopter stability, control and handling characteristics. 'Helicopter Handling Qualities' NASA CP-2219, April 1982.

15) R.W. DuVal, A practical approach to rotorcraft systems identification. 39th AHS National Forum, St. Louis, May 1983.

16) K.H. Fu, M. Marchand, Helicopter system identification in the frequency domain. 9th European Rotorcraft Forum, Stesa, Sept. 1983.

17) M.B. Tischler, J.G.M. Leung, D.C. Dugan, Frequency domain identification of XV-15 tilt rotor aircraft dynamics. AIAA 2nd Flight Testing Conference, Las Vegas, Nov. 1983, (Paper AIAA-83-2695).

18) M.B. Tischler, J.G.M. Leung, D.C. Dugan, Identification and verification of frequency domain models for XV-15 tilt-rotor aircraft dynamics. 10th European Rotorcraft Forum, The Hague, (1984).

19) R.W. DuVal et al, Application of system identification to validation of a helicopter model. 16th Annual Pittsburgh Modelling and Simulation Conference, April 1985.

20) G.D. Padfield, A theoretical model of helicopter flight mechanics for application to piloted simulation. RAE Technical Report 81048, (1981).

21) P.D. Talbot et al, A mathematical model of a single main rotor helicopter for piloted simulation. NASA TM 84281, Sept. 1982.

22) W. Johnson, A comprehensive analytical model of rotorcraft aerodynamics and dynamics. Part 1 - analysis development. NASA TM 81182, June 1980.

23) Prediction of aerodynamic loads on rotorcraft. AGARD CP-334, May 1982.

24) J.S. Winter, G.D. Padfield, S.L. Buckingham, The evolution of ACS for helicopters: conceptual simulation to preliminary design. Active Control Systems-Review, evaluation and projection, AGARD CP 384, 1984.

25) H. Huber, H-J. Dahl, A. Inglsperger, Advanced flight simulation for helicopter development. Helicopter Guidance and Control Systems for Battlefield Support. AGARD CP 359, (1984).

26) G.D. Padfield, Rotorcraft parameter estimation - RAE/NASA collaborative programme. First technical meeting - NASA Ames, Oct. 1981. Unpublished MOD(PE) material (1981).

27) R. Thorne, Summary of RAE Bedford Puma flight mechanics database: Part 1 - parameter identification. RAE Technical Memorandum FS(B) (in preparation).

28) V. Klein, J.R. Schiess, Compatibility check of measured aircraft responses using kinematic equations and extended Kalman filter. NASA TN D-8514, Aug. 1977.

29) G.E.A. Reid, Validation of kinematic compatibility of flight data using parameter estimation methodology. RAE Technical Report 81020, (1981).

30) N.E. Gilbert, M.J. Williams, Preliminary kinematic consistency checking of helicopter flight data. ARL (Australia) Aero Note 414, Jan. 1983.

31) J. Smith, An analysis of helicopter flight mechanics: Part 1 - users guide to the software package HELISTAB. RAE Technical Memorandum FS(B) 569, (1984).

32) G.D. Padfield, J. Smith, An analysis of helicopter flight mechanics: Part 2 - theory for the software package HELISTAB, RAE Technical Report (in preparation).

33) A. Gelb, Applied optimal estimation. MIT Press, Cambridge, Mass, (1974).

34) V. Klein, J.G. Batterson, P.C. Murphy, Determination of airplane model structure from flight data by using modified stepwise regression. NASA TP 1916, (1981).

35) V. Klein, J.G. Batterson, Determination of airplane model structure from flight data using splines and stepwise regression. NASA TP 2126, March 1983.

36) R.I. Jennrich, Stepwise regression. Statistical methods for digital computers, Wiley, New York, 1966.

37) E. Seckel, Stability and control of airplanes and helicopters. Academic Press Inc, New York, (1964).

38) R. Bradley, G.D. Padfield, Design and implementation scheme for an optimal control input device for the RAE Bedford Research Lynx. RAE Technical Memorandum FS(B)
RAE Technical Memorandum FS(B) in preparation.

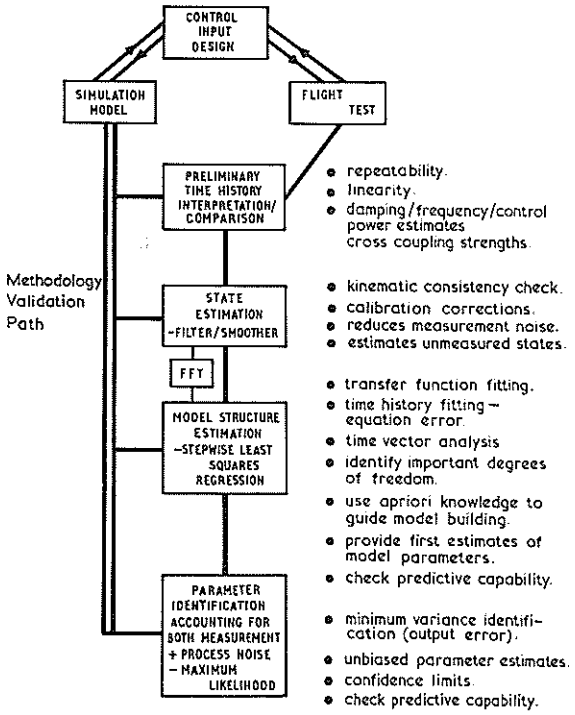

Fig 1 Integrated Methodology for helicopter system identification

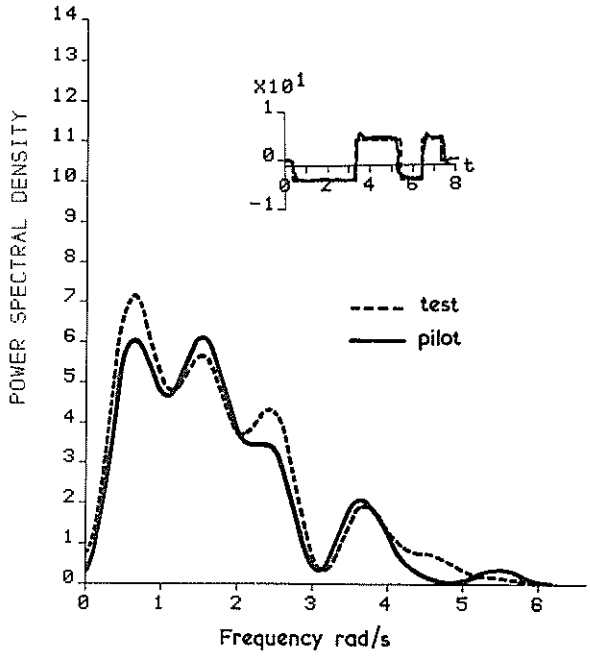

Fig 3 Power Spectrum for 3211 multistep input

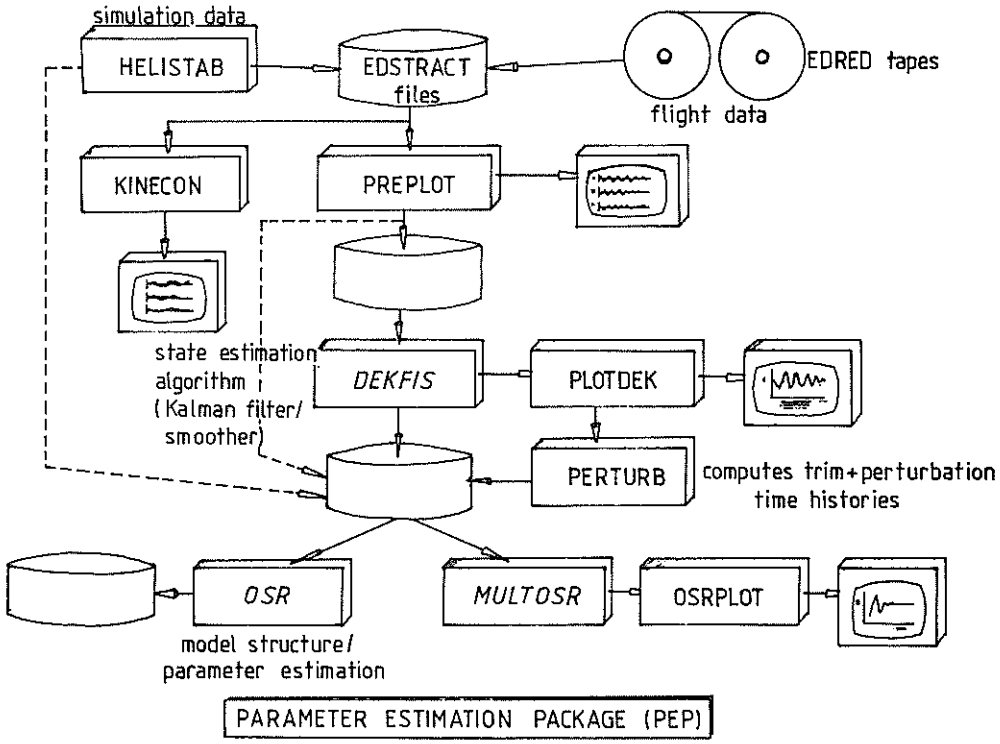

Fig 2 Elements of the Parameter Estimation Package

Fig 4 RAE Bedford Research Puma

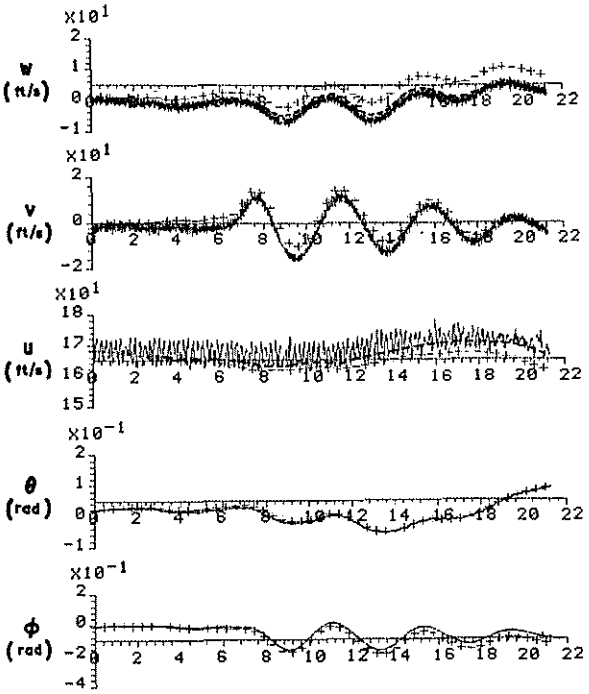

Fig 5 Kinecon results (467/10/11)
- measurements,
+ estimaes before correction,
--- estimates with bias error corrections

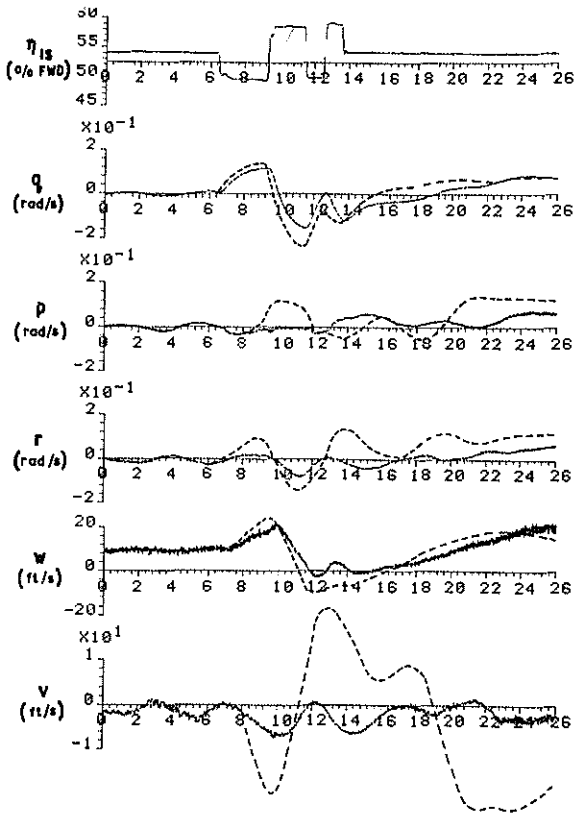

Fig 6 Longitudinal cycle input - comparison of flight measurements (568/03/12) with HELISTAB simulation run (- - -)

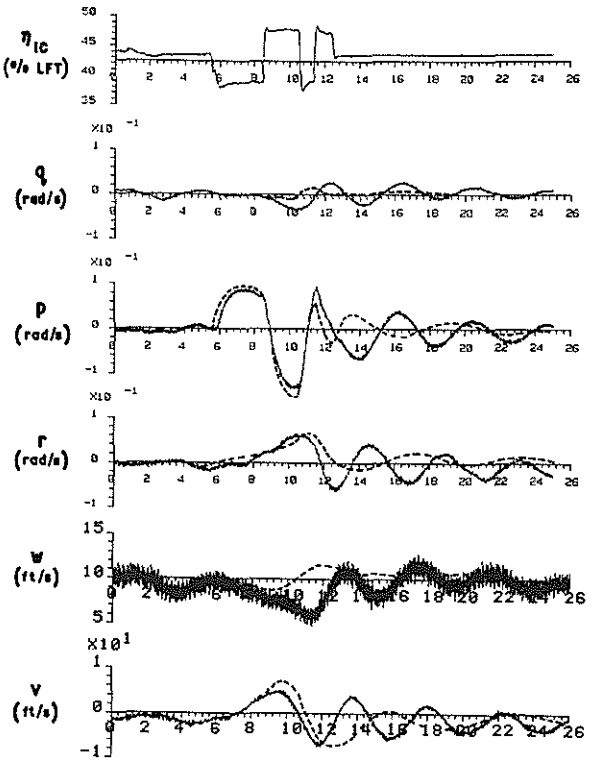

Fig 7 Lateral cyclic input - comparison of flight measurements (568/01/05) with HELISTAB simulation run (- - -)

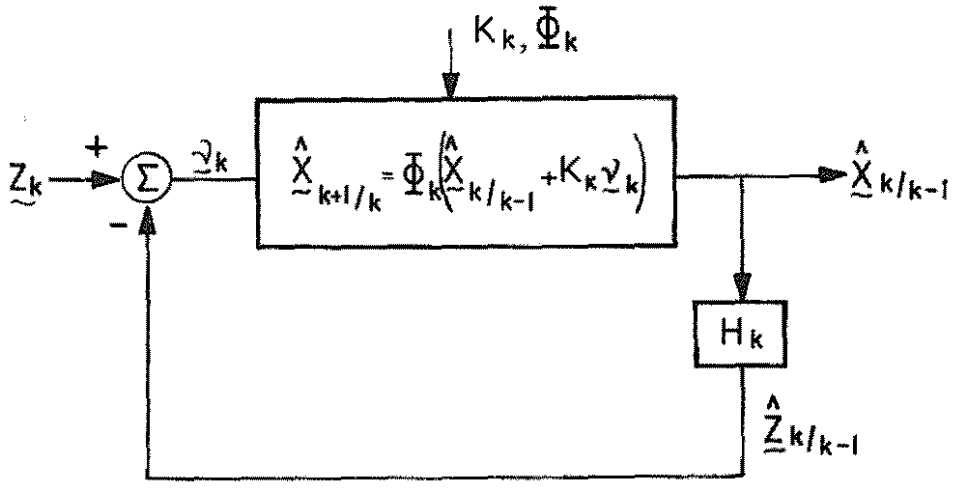

Fig 8 The Kalman filter feedback loop

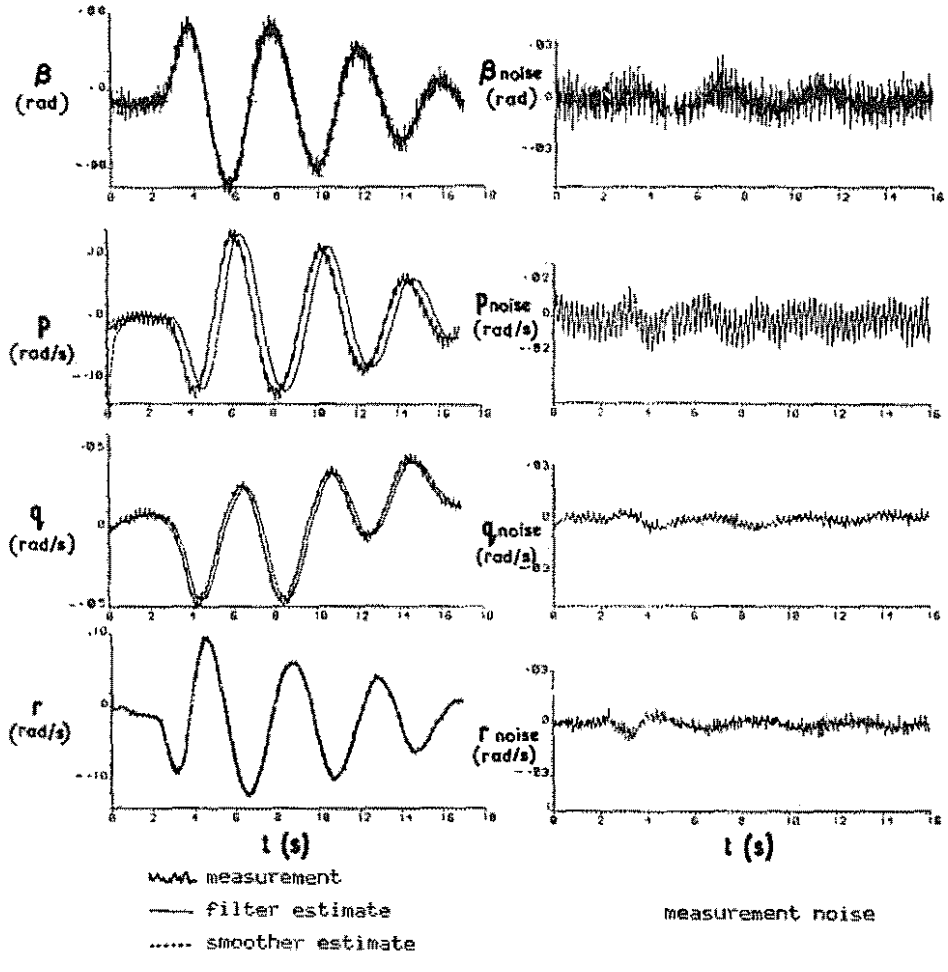

Fig 9 Filter/Smoother state estimates from Run 467/10/11

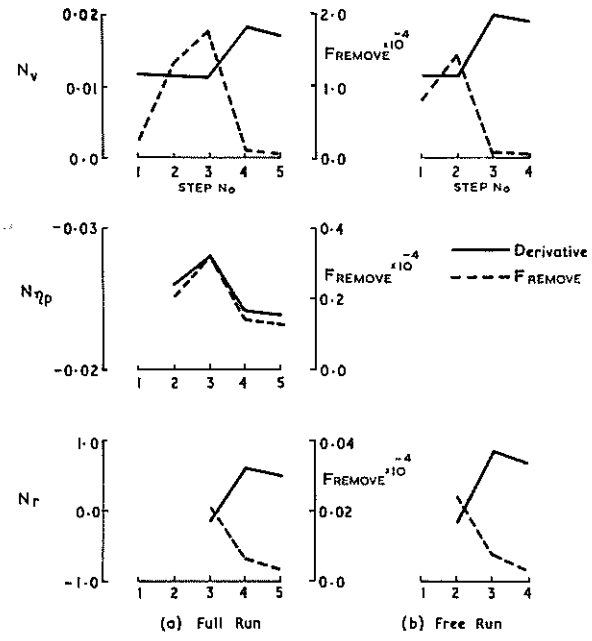

Fig 10 Yawing moment derivatives - Run 467/10/11 (Pedal doublet - 100 kn)

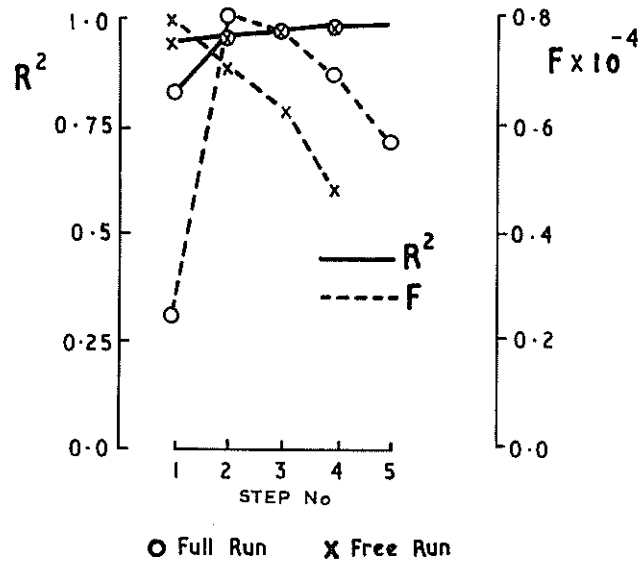

Fig 11 Multiple correlation coefficient (R^2) and total F-ratio for yawing moment derivatives

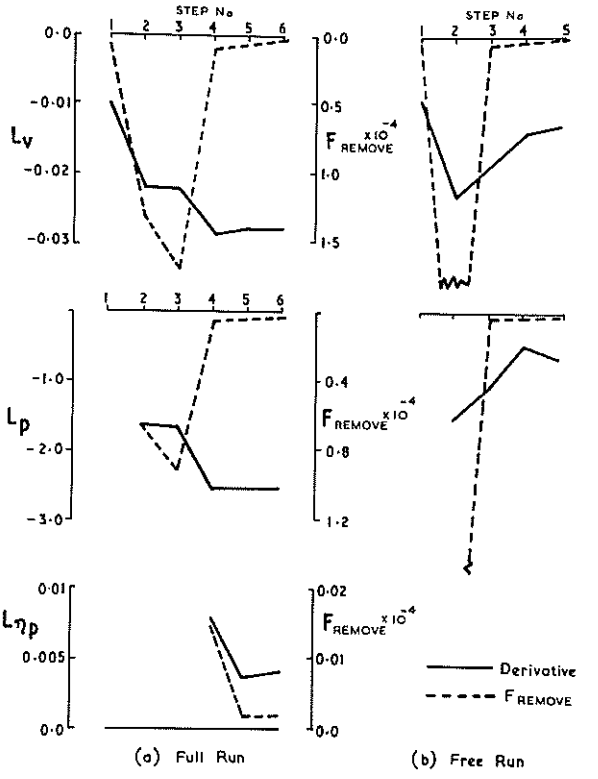

Fig 12 Rolling moment derivatives - Run 467/10/11 (pedal doublet - 100 kn)

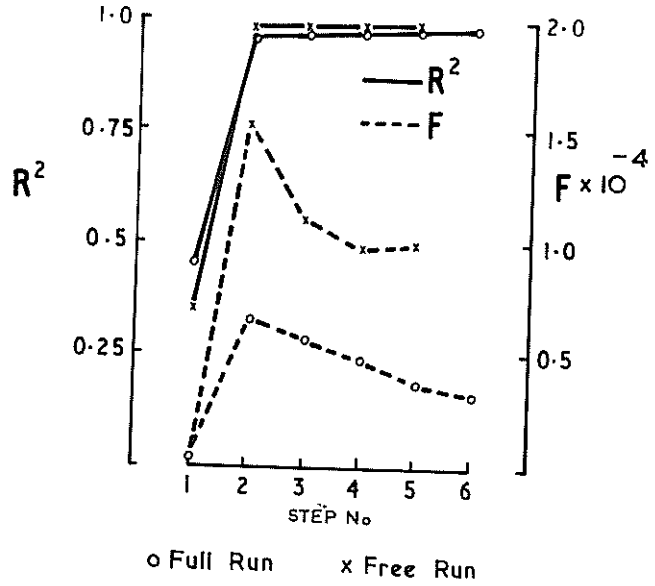

Fig 13 Multiple correlation coefficient (R^2) and total F-ratio for rolling moment derivatives

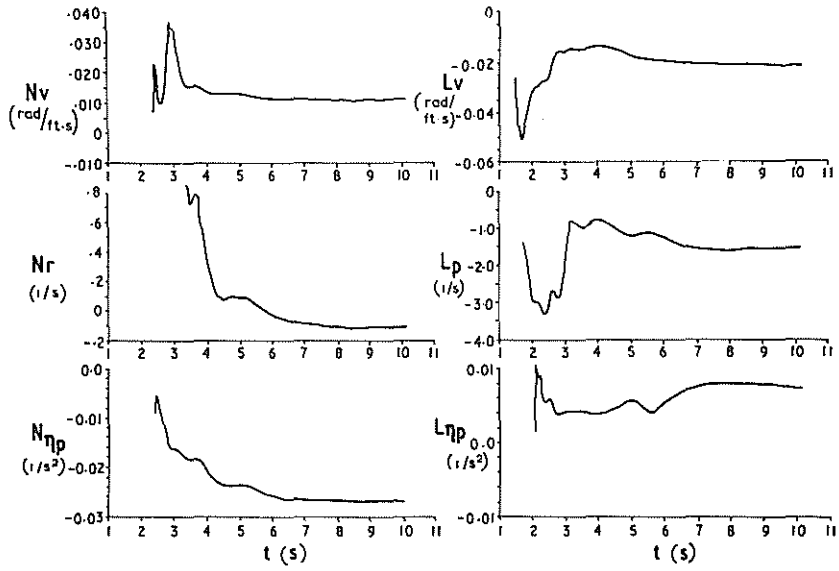

Fig 14 Derivative estimates through multiple stepwise regression

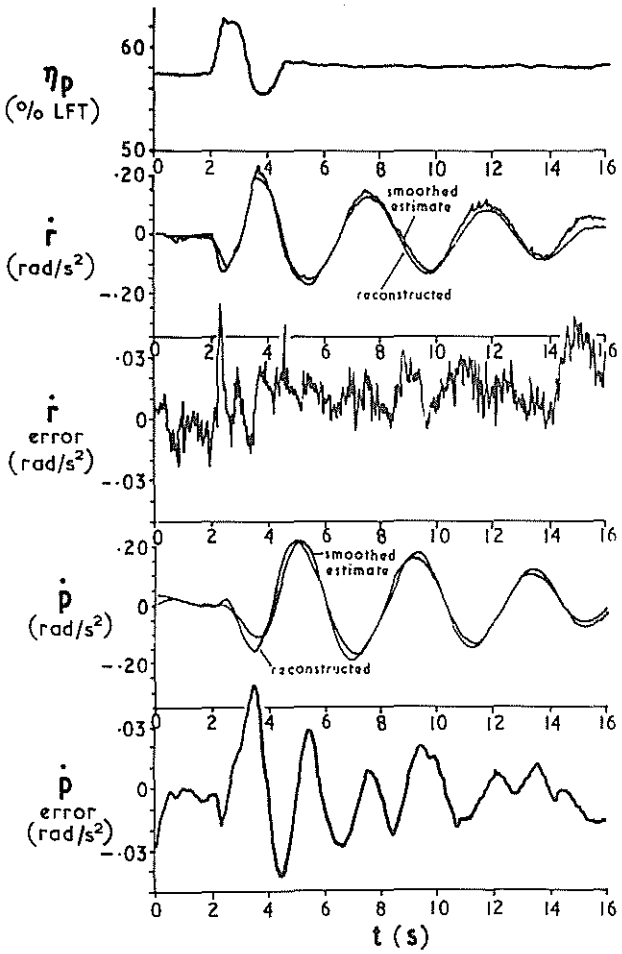

Fig 15 Comparison of smoothed estimates and reconstructed yaw and roll accelerations

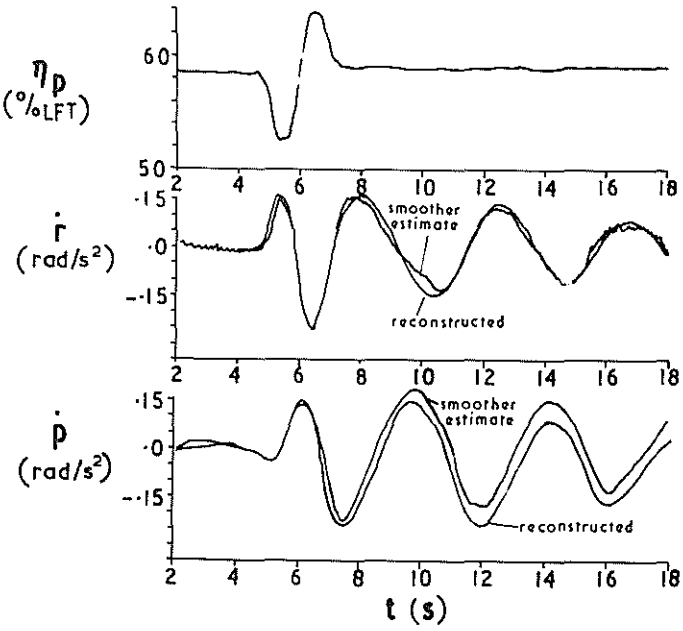

Fig 16 Predictive quality of model structure estimate derived from Run 467/10/11 applied to run 467/11/15

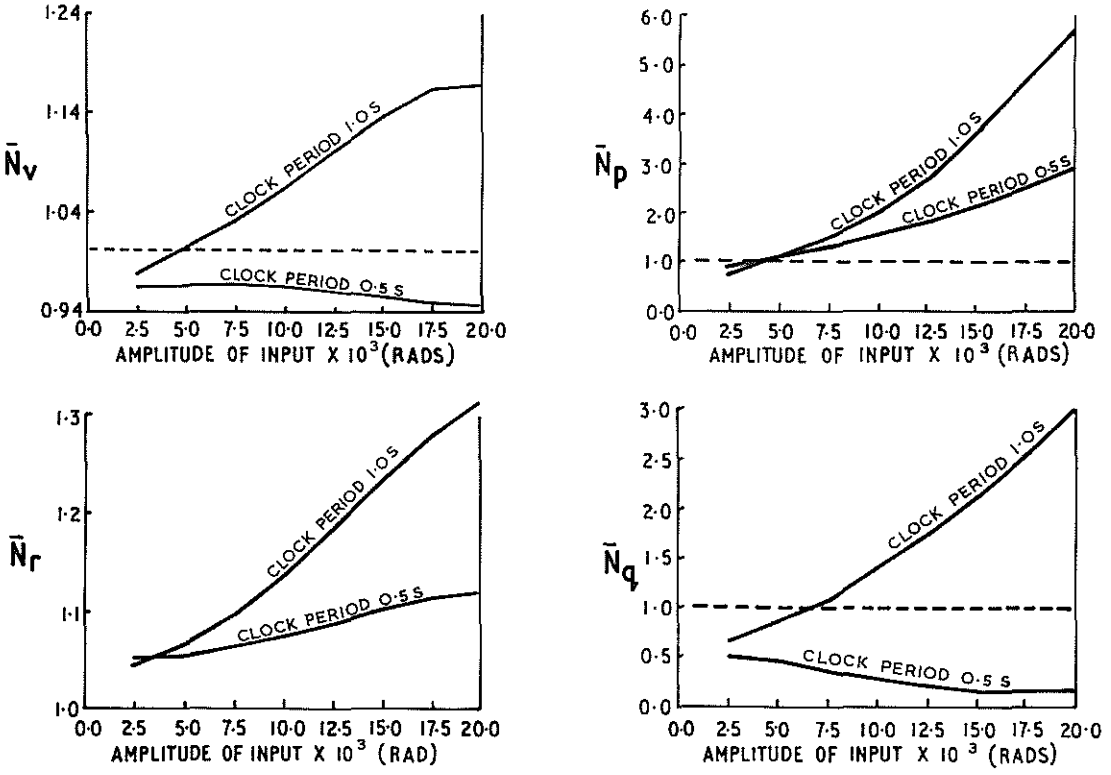

Fig 17 Variation of normalised yawing moment derivatives with input size and clock period: lateral cyclic 3211, HELISTAB Puma 80 kn

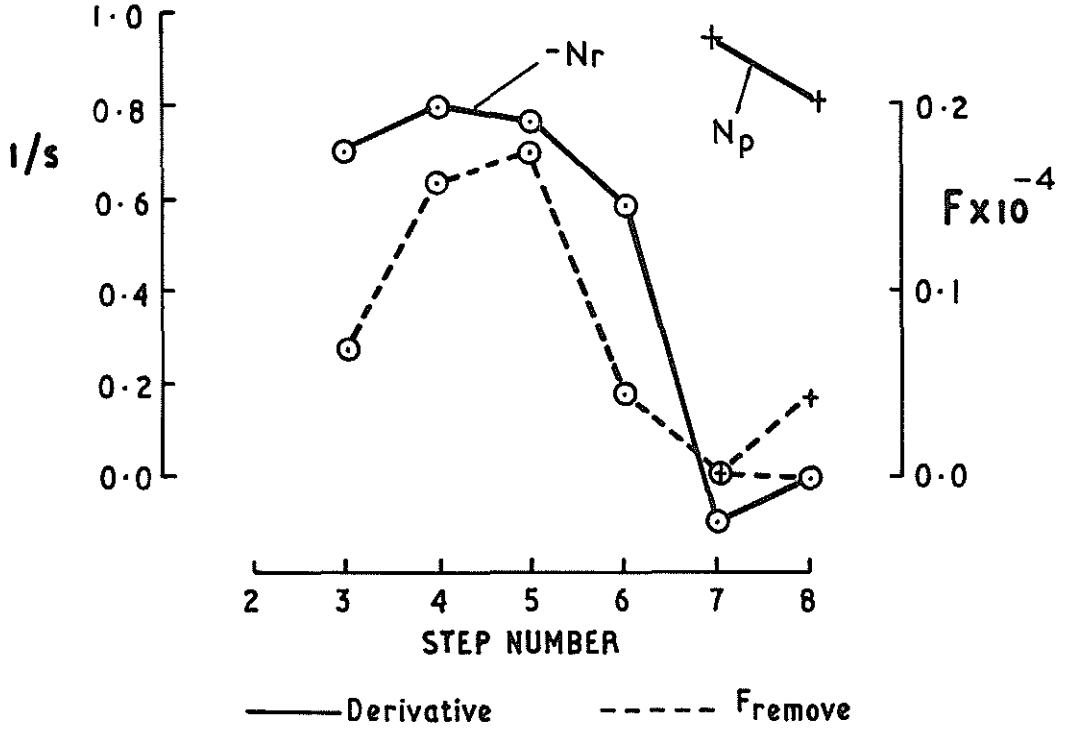

Fig 18 Variation of yaw damping with step number: pedal doublet, HELISTAB Puma 80 kn

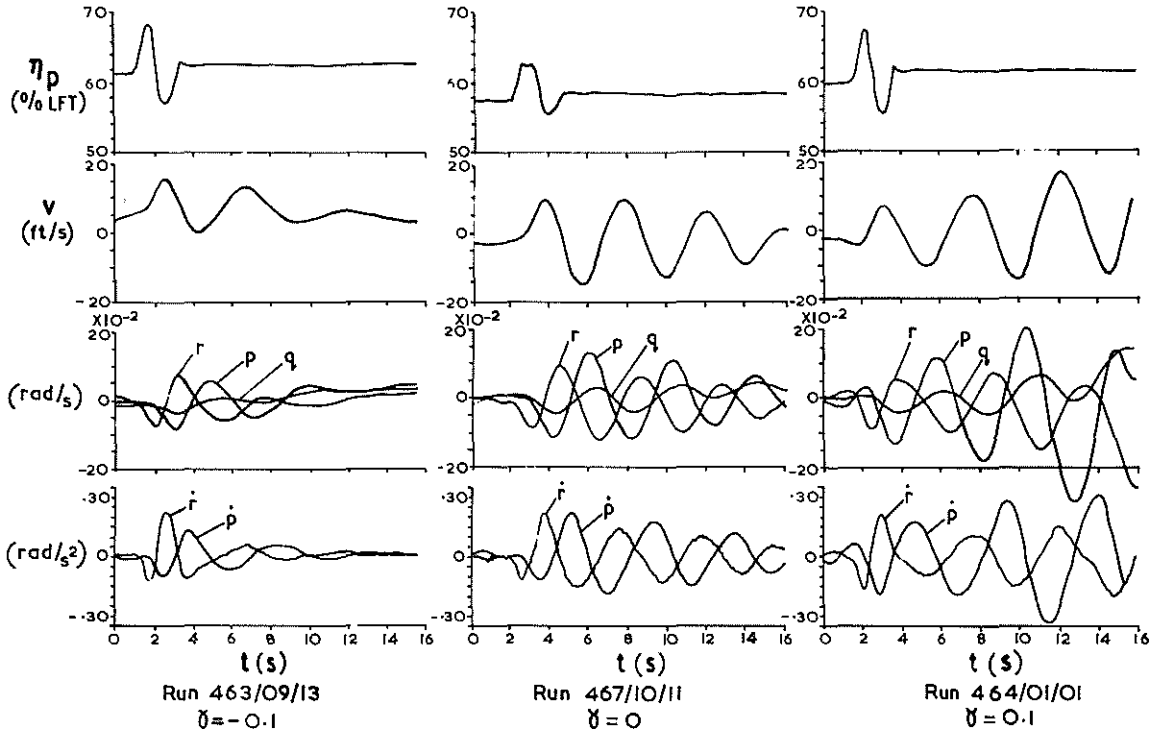

Fig 19 Puma response to pedal doublet (100 kn - descent, level, climb) - smoothed estimates of measurements

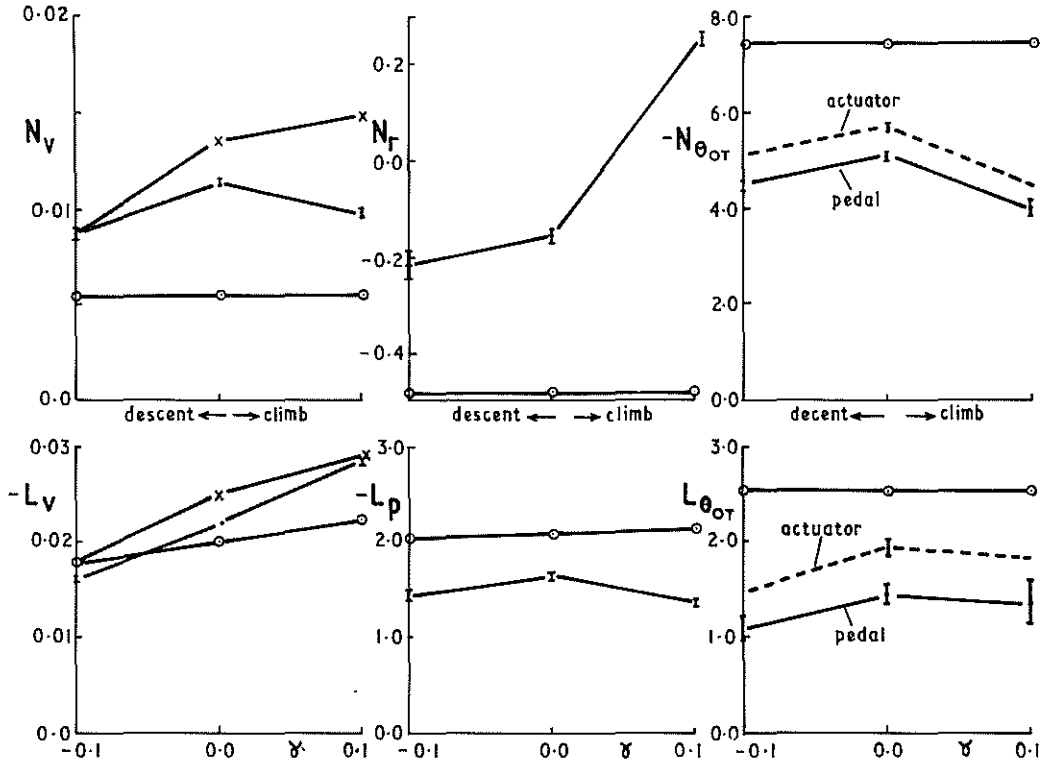

Fig 20 Puma lateral/directional derivatives: PEP estimates (I), steady sideslip tests (x), HELISTAB predictions